Journal of Thermal Analysis and Calorimetry, Vol. 67 (2002) 15–35

EMANATION THERMAL ANALYSIS
Ready to fulfill the future needs of materials characterization

V. Balek[1*], *J. Šubrt*[2], *T. Mitsuhashi*[3], *I. N. Beckman*[4] *and K. Györyová*[5]

[1]Nuclear Research Institute Ře plc, CZ-250 68 Ře , Czech Republic
[2]Institute of Inorganic Chemistry, Academy of Sciences of the Czech Republic, 250 68 Ře , Czech Republic
[3]National Institute for Materials Science, 1-1 Namiki, Tsukuba, Ibaraki 305-0044, Japan
[4]Department of Chemistry, Moscow State University, 199234 Moscow, Russia
[5]Department of Inorganic Chemistry, P. J. Šafárik University, Moyzesova 11, 04154 Košice, Slovak Republic

Abstract

The paper reviews the actual state of the development and use of emanation thermal analysis (ETA). Examples of its recent applications are presented. The advantages of ETA in the microstructure characterization of materials under *in situ* conditions of their heat treatment are outlined.

Keywords: emanation thermal analysis, microstructure, sintering, solid state transitions, surface roughness annealing

Introduction

Emanation thermal analysis (ETA) [1] is based on the measurements of the release of inert (radioactive) gases from previously labelled solid samples, during heating under controlled conditions. The release of inert gases makes it possible to monitor changes in surface area, morphology and crystal structure of solid samples under *in situ* conditions of their heat treatment. The inert gas atoms serve in ETA as the nanostructure probe of materials. The processes of the interaction of solids with gases, liquids or other solid components were investigated by ETA in numerous systems. The high sensitivity of ETA towards order–disorder changes taking place during structure transitions, sintering, weathering of rocks or corrosion of solid surfaces has been advantageously used. Moreover, this method gives a supplementary insight into processes of radiation damage, alteration and degradation of materials surfaces. ETA results usually complement results of DTA, TG, XRD, surface area, porosity, optical and electron microscopy characteristics of the samples.

* Author for correspondence: E-mail: bal@ujv.cz

1418–2874/2002/ $ 5.00

Akadémiai Kiadó, Budapest
Kluwer Academic Publishers, Dordrecht

In recent years the theoretical background of ETA has been upgraded, the methods for the evaluation and for interpretation of ETA results were updated in order to meet the requirements for the computer treatment of the experimental data. The aim of this paper is to present the actual state of art of the emanation thermal analysis as a less common method of thermal analysis and to outline the possibilities of its use in the solution of various problems of materials research.

Principles of emanation thermal analysis (ETA)

In ETA the release of the inert gas atoms is measured from previously labelled samples heated or cooled under controlled conditions. Most of the solids to be investigated by ETA do not naturally contain inert gas and it is necessary to label them with a trace amount of the inert gas. Various techniques can be used for the introduction of inert gas atoms into the samples to be investigated [1].

Implantation of accelerated ions of inert gases

This technique has often been used for labelling samples to be investigated by ETA. The amount of inert gas introduced and its concentration profile depend on the energy of ion bombardment and the properties of the labelled matrix. A number of techniques can be used for inert gas ion bombardment [1]. A defined ion beam can be produced using a magnetic separator. A versatile low-cost technique for the sample labelling in a low-temperature plasma produced by a high-frequency discharge was proposed by Jech [25].

Introduction of parent nuclides as a stable source of inert gas atoms

This method has been advantageously applied when radon ^{220}Rn is used in the characterization of surface and morphology changes of solid samples, serving as inert gas probe in ETA. Thorium ^{228}Th (half-life 1.9 years) represents a quasi-permanent source of radon ^{220}Rn (half-life 55 s). The release of radon atoms from the samples can be measured continuously, under *'in situ'* conditions of the sample treatment [1]. Trace amounts of thorium ^{228}Th can be introduced into the sample by co-precipitation during the sample preparation from a solution or by adsorption on the surface of the sample. ^{220}Rn is formed by spontaneous α-decay according to the scheme:

$$^{228}\mathrm{Th} \xrightarrow[T_{1/2}=1.9\ \mathrm{y}]{\alpha} {}^{224}\mathrm{Ra} \xrightarrow[T_{1/2}=3.8\ \mathrm{d}]{\alpha} {}^{220}\mathrm{Rn} \xrightarrow[T_{1/2}=55\ \mathrm{s}]{\alpha} \qquad (1)$$

The above α-decay nuclear reactions give rise to the radium and radon nuclides, possessing the recoil energy of 85 keV per atom. This energy has been used for the incorporation of the radon atoms into the near surface layers of the solid sample. The recoiled radon atoms penetrate several tens of nanometers into the sample, depending on the composition of the target materials. The concentration profiles of ^{224}Ra and ^{220}Rn can be calculated by Monte Carlo method and using TRIM code [2]. For exam-

ple, the calculated values of the recoil ranges in titania (anatase) are: for ^{224}Ra: 21.1 nm (straggling 6.1 nm) and for ^{220}Rn 27.0 nm (straggling 6.5 nm), respectively. Therefore, the penetration depth of ^{220}Rn atoms in the anatase near surface layers is up to 67.3 nm. The number of vacancies produced by ^{224}Ra and ^{220}Rn recoiled ions is 491 and 485, respectively. In SiC the recoil depths of ^{224}Ra and ^{220}Rn ions were calculated as: 37.7 nm (straggling 3.9 nm) and 38.2 nm (straggling 3.8 nm) respectively. Consequently, the radon atoms penetrate into the near surface layers of SiC to the maximum depths of 83.6 nm. By this way the parent nuclides of ^{228}Th and ^{224}Ra serve as 'recoil ion implantators' of the radon atoms. The high amount of ^{220}Rn is situated next to the surface having the descendent character of the concentration profile from the surface. This ensures the high sensitivity of ETA to the changes of surface roughness and microstructure in the near surface layers.

Measurement of inert gas release during ETA

In ETA measurement, a selected gas (e.g. air, nitrogen) carries the radioactive atoms of the inert gas released by the sample into a detector for the inert gas. For example, to measure the α-activity of radon, a scintillation counter, ionisation chamber or semiconductor detectors can be used. Geiger–Müller tubes were used for β-activity measurements of ^{85}Kr. γ-activity of xenon ^{133}Xe nuclide can be measured by γ-spectrometer. The stable nuclides of inert gases are usually measured by mass spectrometer.

The sample is situated in a furnace being overflowed by a constant flow rate of the carrier gas. To ensure optimum conditions for a direct comparison of ETA data with results obtained by other thermal analysis methods, devices were constructed to provide simultaneous measurements of additional parameters. The equipment for simultaneous measurements by ETA, DTA, TG/DTG or dilatometry [3] produced by Netzsch Ltd., Germany, ensures the optimal conditions for direct comparison of the results.

Background considerations underlying the use of ETA

The solubility of inert gas atoms, such as radon, in inorganic solids is small. The inert gases are trapped at lattice defects such as vacancy clusters, grain boundaries and pores. The defects in the solids can serve both as traps and as diffusion paths for the inert gas. A survey of the influence of various factors on the migration of inert gases in solids is given in [1].

In instances when the inert gas atoms are incorporated into the solids without their parent isotopes, diffusion in the matrix is the main mechanism for the gas release from solids. In instances when the parent nuclides of the inert gas are incorporated into the solid samples as a permanent source of the inert gas, the recoil mechanism of the inert gas release should be taken into account in addition to the diffusion.

Various mechanisms were considered in the mathematical description of the radon release from solids in the series of the papers [4–18] devoted to the development of ETA theory.

The mathematical description of the probability of the release of inert gas atoms incorporated into the solids was based on the following considerations:

(i) Parent nuclide(s) of the inert gas are incorporated into the solid. The inert gas is formed by radioactive decay of the parent nuclide and may escape from the solid either by recoil energy ejection or by any one of several types of diffusion processes.

(ii) When the radium atom lies close to the surface of the grain of the solid, the recoil energy (85 keV per atom) that the radon atoms gain during the decay of the parent atoms may be sufficient to eject the gas atoms from the grain. Alternatively, the radon atoms may escape by diffusion before they undergo the decay.

(iii) The term emanating power E is defined [1] as the ratio of the rate of inert gas release to the rate of gas formation in the solid.

(iv) The inert gas (radon) release due to recoil, diffusion in open pores and diffusion of inert gas in the solid matrix have been considered as mechanisms contributing to the release of radon from the sample.

Principal consideration of the surface area diagnostics based on the ETA measurements

It is supposed that ^{228}Th and ^{224}Ra do not migrate in the solid. If no chemical or physical changes take place in the homogenous solid studied under quasi-stationary conditions the total emanating power E_{TOTAL} is composed by three terms, namely E_R, E_P and E_S.

The term E_R of the emanating power due to recoil can be expressed as

$$E_R=K_1S_1 \tag{2}$$

where K_1 is a temperature-independent constant, that depends on the path of the recoiled gas atoms in the solid, and S_1 is the external surface area (involving the surface roughness) of the sample. The path of recoiled atoms of radon is dependent on the 'nuclear stopping power' of the sample material (for details see [1], p. 29). Expression (2) is valid for isolated grains of the solid that are larger than the path of the recoiled radon atoms. For finely dispersed solids, the constant K_1 depends on the dispersity and morphology of the sample, on the shape and size of the grains.

The term E_p of the emanating power due to the inert gas diffusion in the intergranular space and open pores can be expressed as

$$E_P=K_2S_2 \tag{3}$$

where K_2 is a constant that depends on temperature, and S_2 is the internal surface area of the sample.

The term E_S of the emanating power due to the inert gas diffusion in the solid matrix of the sample can be expressed as

$$E_S=K_3\{(D/\lambda)^{1/2}\}S_3 \tag{4}$$

where K_3 is a temperature-independent constant, $(D/\lambda)^{1/2}=L_D$ is diffusion length, D is diffusion coefficient of radon in the solid sample, $D=D_0\exp(-Q/2\boldsymbol{R}T)$, Q is the activation energy of inert gas diffusion in the solid matrix, $\boldsymbol{R}$ is the molar gas constant, T is

the absolute temperature and S_3 is the area representing the sum of the cross sections of all diffusion paths, such as dislocations, grain boundaries, etc.

The total emanating power E_{TOTAL} measured experimentally can be expressed as a sum of the terms

$$E_{TOTAL}=E_R+E_P+E_S \quad (5)$$

It is to point out that the surface area resulting from E_R, E_P, and E_S values resp. may differ. Each of the terms characterises different properties of the surface and near surface layers of the sample. In order to determine the values of individual terms E_R, E_P and E_S the measurements by ETA are usually carried out at various temperatures and evaluated by means of the models designed for the description of the radon mobility in the respective types of solids (porous, non-porous, finely dispersed), etc. For the characterisation of microstructure of highly disordered solids the diffusion of radon is used as the probe for diffusion structure analysis of the samples. Consequently, ETA makes it possible to obtain a more detailed insight into surface area and their changes, into the changes of the microstructure of the near surface layers labelled by radon atoms.

Principal considerations concerning the use of radon as diffusion structural probe of solids

(i) The materials formed during thermal decomposition of solids contain various types of defects (irregularities of the structure), which might serve as channels for radon diffusion.

(ii) The changes in radon diffusion mechanism taking place during heating may reflect the microstructure changes of the intermediate products. Taking into account that the diffusion length L_D of radon increases with the temperature it is supposed that the thickness of the near surface layers to be characterized by ETA on heating can vary from the depth of several crystallographic distances (approx. 1 nm) to 100 nm, into which radon atoms were incorporated by recoil.

(iii) During ETA experiments the rate of radon released from solids is measured. It is considered that in the range from room temperature up to approximately $0.2T_m$ (T_m is melting temperature in absolute scale) the radon release rate due to the diffusion along the near surface irregularities in the depth of several crystallographic distances(called 'damage diffusion' takes place. Annealing of the surface roughness and irregularities in this near surface layers is characterised as the decrease of the radon release rate in the corresponding temperature range.

It is supposed that in the temperature range 0.2–0.5 T_m the diffusion of radon in the surface layers up to 100 nm from the surface takes place. The 'single jump diffusion' mechanism is considered for radon diffusion in this temperature range. The decrease of E in this range observed experimentally on ETA curves may indicate such processes as the thermal annealing of the microporosity, collapse of inter-laminar structure and sintering. The abrupt decrease of the radon release rate observed on ETA curves can be described in the modelling by symmetric or asymmetric descend-

ing functions. The experimental verification of the used model is necessary in every case. In the temperature range above $0.5T_m$ the radon diffusion length increased, so that it exceeds the sum of the recoil penetration depths for Ra and Rn atoms. For elevated temperatures the radon diffusion length in the thermally stable solids may increase up to several μm [16]. Consequently, ETA makes it possible to characterize the microstructure changes taking place at elevated temperatures even in the bulk of the solid.

(iv) The function $\Psi(T)$ was suggested for the description of the change of number of defects, which can serve as traps for radon atoms. The number of radon diffusion paths is changing during heating of the sample.

In the temperature range approximately up to $0.2T_m$ the function $\Psi(T)$ describes the change of number of the near surface defects serving as traps for radon atoms. During heating to temperatures exceeding this range the radon atoms escaped from the traps as the result of their annealing and diffused to the sample surface. The decrease of E observed on the ETA-curve characterised the near surface defects annealing process.

In the temperature range $0.2–0.5T_m$ $\Psi(T)$ describes the annealing of a surface roughness and/or the collapse of porous structure. It may correspond to the function describing the changes of surface area or opened porosity determined by BET- method.

(v) In the modelling of ETA curves it is suggested to use the product $D(T)\Psi(T)$ for the description of the changes of the emanating power due to radon diffusion in the sample where annealing of the defects, phase changes or other solid state transitions take place. In this case the function $\Psi(T)$ reflects the change of the number of radon diffusion paths during heating. The function $D(T)$ reflects the change of radon diffusion permeability of the average radon transport path. Thus, the product $D(T)\Psi(T)$ represents the change of radon permeability in all diffusion paths participating in process.

(vi) If solid state transitions in bulk of materials take place, a series of intermediate metastable structures may be formed, considerably varying in the number of radon migration paths, in the permeability of radon diffusion paths as well as in the area of surface accessible for gas release. It was observed that these processes essentially influence the shape of ETA curve. If several consecutive solid state changes take place during sample heating, several peaks may be observed on the ETA curve. In order to evaluate ETA results obtained during heating of such solids, different mechanisms for radon diffusion were considered.

Following mechanisms for radon diffusion were considered in the modelling

(i) Parallel diffusion in two channels

(ii) Parallel diffusion supposing an exchange of inert gas atoms between channels

(iii) Parallel diffusion supposing an exchange of inert gas atoms between channels and the change of defect concentration

(iv) Consecutive diffusion mechanism in several channels

The mechanism of consecutive diffusion assumes, that in an interval of temperatures $T_1 \leq T \leq T_2$ radon is diffusing in the stable structure of the initial material, which is

characterised by the parameters D_{10} and Q_1 (cf. Eq. (5)). At temperatures $T_3 \leq T \leq T_4$ radon is diffusing in the newly formed structure and characterised by D_{20} and Q_2. In more complex models of consecutive diffusion the smooth transition from one structure of a material to another through a series of intermediate states is taken into account. Monotonous functions of transition from D_{10} to D_{20} and from Q_1 to Q_2 in this case have been used in the modelling [1, 4, 16, 17].

In the presence of solid state transitions in the solid, the temperature dependence of emanating power E_{TOTAL} can be schematically expressed as:

$$E_{\mathrm{TOTAL}} = E_{\mathrm{R}} + \sum D_{\mathrm{n}}(T)\Psi_{\mathrm{n}}(T) \tag{6}$$

where E_{R} is the emanating power due to recoil. The emanation power due to radon diffusion is determined by $D_{\mathrm{n}}(T)$ and $\Psi_{\mathrm{n}}(T)$ functions, characterising the diffusion and microstructure processes in the respective temperature intervals.

The temperature dependencies of radon diffusion coefficient $D_{\mathrm{n}}(T)$ can be considered as growing functions, whereas $\Psi_{\mathrm{n}}(T)$ (determining the annealing of diffusion paths) as descending functions. Consequently, peak-like parts are resulting in the mathematical modelling of the temperature dependencies of emanating rate E.

In general, the shape of ETA curve depends on a number of diffusion paths serving for the gas release; $D_{\mathrm{n}}(T)$ are the functions characterising the permeability of the transporting paths and $\Psi_{\mathrm{n}}(T)$ are characterising the microstructure changes in the solids. The selection of $D_{\mathrm{n}}(T)$ and $\Psi_{\mathrm{n}}(T)$ functions in the modelling is determined by the mechanisms of the chemical or physical processes taking pace in the solid during heating [16].

Advantages of ETA use

The theoretical considerations summarised above indicate that ETA can be used in the investigation of processes taking place in solids or on their surfaces. Any process in a solid or its phase boundaries leading to changes in either the surface and/or changes in the inert gas diffusion becomes observable from ETA measurements.

The information obtained by ETA is usually compared with results DTA, TG and other methods. In contrast to DTA and TG, ETA made it possible to investigate processes that are not accompanied by thermal effects or mass changes, such as of sintering of powdered or geleous samples, which has been so far impossible to study by means of common dilatometry [19–22].

In contrast to X-ray diffraction spectrometry, ETA made it possible to reveal even fine changes in poorly crystalline or amorphous solids. In contrast to adsorption measurements of surface area, the continuous monitoring of surface changes at elevated temperatures was carried out by ETA, without the necessity of interrupting the heat treatment and cooling the sample to liquid nitrogen temperature. For this reason, ETA indicated the formation of intermediate phases with metastable surfaces directly at elevated temperatures, which was not possible to observe by adsorption measurements at low temperatures. Nevertheless, the calibration of E values with respect to the surface area characterised by BET method is requested. For example, ETA made

it possible to reveal differences in the morphology and behaviour of samples prepared by sol-gel technique at different conditions (i.e. the composition of feed solutions, conditions used for gelation, ageing, drying and heat treatment of gels). The kinetics of surface area changes of defects annealing or pore sintering, i.e. the kinetics of morphology changes of solid samples, can be evaluated from ETA results obtained under *in situ* conditions of isothermal or non-isothermal treatment.

Moreover, the inert gas release measurements during cooling of thermally treated samples can be used for the characterisation of the degree of density attained by the previous thermal treatment [22]. The radon diffusion parameters serve as quantitative characteristics of the inert gas mobility.

ETA has been used in the study of such solid state processes as the thermal decomposition of solids and chemical reactions in solids and on their surfaces, including solid–gas, solid–liquid and solid–solid interactions. ETA results were used in the optimisation of conditions for the preparation and thermal treatment of advanced ceramic materials [4], as well as in testing properties of hydraulic binders during their hydration at requested temperature and at presence of admixtures [23, 24].

Moreover, by applying different radioactive labelling techniques of either the surface alone or the volume of solids, the processes taking place in the surface and in the bulk of the sample have been discerned by ETA. This is especially advantageous when studying the thermal behaviour of thin films or coatings on substrates. By labelling the thin films to a depth not exceeding its thickness, ETA gave information concerning the thin films as such without the influence of the substrate. On the other hand, when the interaction of the thin films with the substrate during heating is to be investigated, a deeper inert gas implantation can be used.

The high sensitivity of ETA to chemical interactions between solid surfaces and aggressive agents made it possible to reveal the very beginning of corrosion reactions. The durability of materials towards aggressive liquids and gases, as well as the effectiveness of protecting coatings, was tested by means of ETA.

In addition, ETA measurements made it possible to obtain information about the diffusion parameters of the inert gas in the solid. The diffusion coefficient D and the activation energy Q of the inert gas diffusion were evaluated from ETA results. The inert gas diffusion parameters in inorganic and organic materials were used for the characterisation of the transport properties of materials.

Examples of materials characterisation by means of ETA

Diagnostics of the defect state of solids

Inert gas atoms situated on the natural and/or artificial defects in solids, produced for example by ion bombardment, neutron irradiation or mechanical treatment, can be released as the result of diffusion and the annealing of defects. Inert gas diffusion parameters evaluated from ETA measurements characterised the mobility of inert gases in the solids [1]. It was shown that the mobility of inert gas atoms in the ionic crystals differs in various crystallographic directions, owing to the channelling effect. The

mobility of the inert gases (e.g. the value of activation energy of inert gas diffusion) was used [25–28] as a parameter characterising the defect state of an ionic crystal lattice. It reflected the formation and the annealing of the metamict phases. The temperature of the recrystallisation of the metamict phases was evaluated from the effect on the ETA curve. A number of alkali halides, alkali earth halides, silicates and oxides, have been investigated by ETA from this viewpoint [1].

Assessment of thermal and chemical history of inorganic materials

Thermal and chemical history of inorganic materials can be assessed from ETA results measured during heating and subsequent cooling of heat-treated samples.

Figure 1 shows as an example the results of ETA for iron(III) oxide samples prepared from four different iron salts previously labelled by radon parent nuclides, ^{228}Th and ^{224}Ra and heated up to 1100°C in air. The values of the activation energies Q of radon

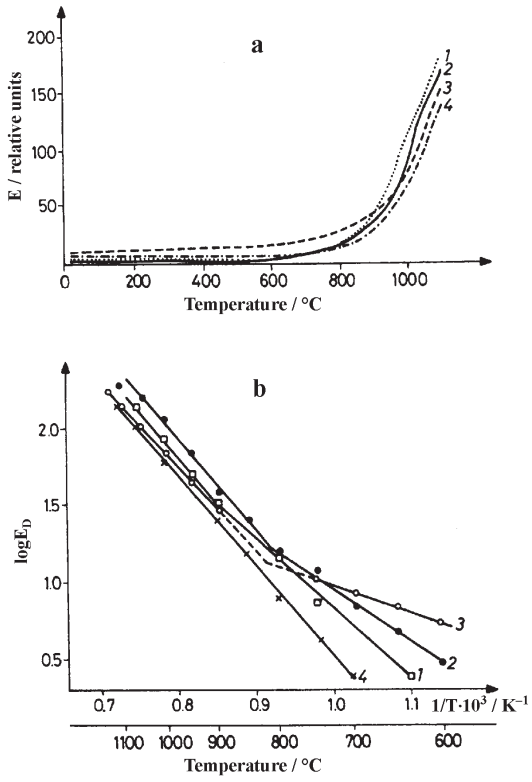

Fig. 1 ETA curves of iron(III) oxide samples prepared by heating of various iron salts to 1100°C; iron(II, III) carbonate (curve 1); iron(II) sulphate (curve 2); Mohr's salt (curve 3) and ferrous(II) oxalate (curve 4); a – as dependence of E *vs*. T; b – as dependence of logE_D *vs*. l/T [29]

diffusion calculated from the $\log E_D$ *vs*. $1/T$ relationship in the temperature range 600–750°C, Q=46, 79, 117 and 136 kcal mol^{-1}, correspond to the iron(III) oxide samples prepared by heating Mohr's salt, iron sulphate, iron carbonate and iron oxalate, respectively. The highest values, corresponding to iron(III) oxide from oxalate, indicated the relative lowest reactivity in the series of the samples tested [29]. The influence of the thermal and chemical history on the active state of powdered iron(III) oxides prepared by heat-treatment of various iron salts was determined from the experimental results of ETA at temperatures 600–750°C, i.e. lower than $0.5T_m$. In this temperature range the activation energy of radon diffusion reflects the concentration and type of non-equilibrium defects remaining in the structure of iron(III) oxides after the decomposition of initial iron salts used for the preparation of the oxide samples. In this way, ETA made it possible to characterize the differences in 'the structure memory of solids' [1]. ETA was used to characterize the differences in the thermal behavior of materials prepared under different experimental (technological) conditions. In our study [30] we characterized the differences in the thermal behavior during heating of SiC powders under *in situ* conditions of the heating in argon. The differences in the microstructure changes of the samples of SiC ultrafine powders (size 20 nm) prepared by laser assisted synthesis from silane hydrocarbon mixture, samples of submicron SiC powder and SiC whiskers, resp. were revealed by means of ETA.

The decrease in sinterability, reactivity or catalytic activity of iron oxide samples was predicted from the increased value of the activation energy of radon diffusion. The structure defects, affecting the active state of solids, were characterised in this way [1, 29].

Microstructure development of oxide powders and layers during heating their precursors

Ruthenium oxide RuO_2 is well known as a corrosion resistant material possessing a metal-like conductivity and excellent thermal resistance characteristics. It has also been proposed as the catalyst for several catalytic reactions of technological and environmental importance. ETA characterized the microstructure development of ruthenia based materials during heating of their precursors in the temperature range 20–600°C [31]. A good agreement of ETA results with the results of TG, DTA, surface area, TEM and XRD was found.

ETA was used in the preparation of titania based photosensitive materials by heating of hydrous titania and titania containing 10% of ruthenia [32]. As it follows from the comparison of ETA results of TG, DTA, XRD, TEM, and surface area [32] the ETA made it possible to monitor the microstructure changes under *in situ* conditions of heat treatment and to determine the optimised conditions for the preparation of photosensitive materials based on titania. ETA results of $TiO_2 \cdot nH_2O$ and $(TiO_2)_{0.9}$–$(RuO_2)_{0.1} \cdot nH_2O$, used as precursors for titania based materials, are presented in Fig. 2.

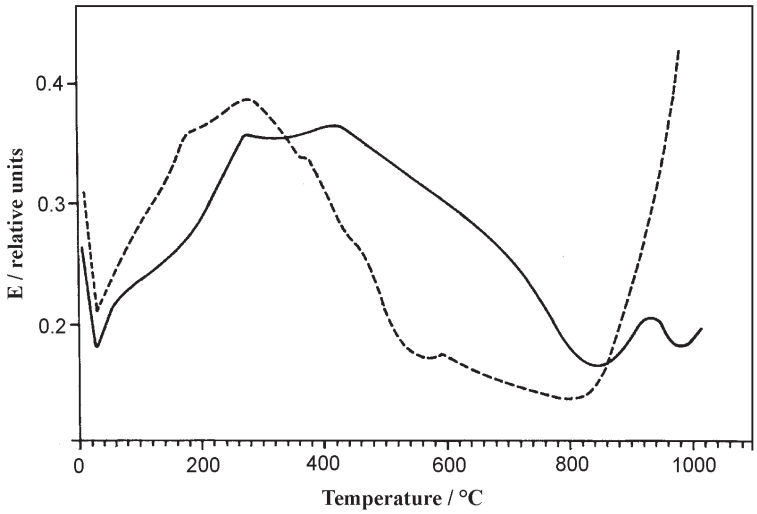

Fig. 2 ETA curves measured during heating of hydrous titania (full line) and hydrous titania containing 10% of ruthenia (dotted line). Heating in argon at the rate 5 K min^{-1}

The surface area of the sample heated to 300°C was S=148.4 m^2 g^{-1}, it decreased to S=89.7 m^2 g^{-1} after heating to 500°C. At the temperatures of 400 and 500°C, resp. a partially crystalline anatase phase was detected by XRD. In the titania sample heated to 800°C, well developed crystals of anatase of the size ~0.1 μm were observed (S=41.6 m^2 g^{-1}).

ETA characterised the microstructure changes of the hydrous titania during heating as follows (full line in Fig. 2). The increase of Rn release rate, E, in the temperature interval 20–300°C reflected the process of the surface liberation from water. In the temperature interval 300–420°C no significant changes of E were observed. On further heating to 800°C a decrease in E corresponded to the growth of the primary grains of anatase and its subsequent crystallisation. ETA results were in agreement with the surface area, XRD and TEM characteristics of titania heated to selected temperatures in the range 400–800°C [32].

At 850°C the onset of the enhanced Rn release by thermal diffusion was observed. The decrease of E values starting at 910°C corresponded to the intense growth of the primary grains, accompanying the phase transformation of anatase to rutile. At further heating above 980°C the E increase characterised the diffusion of Rn in the rutile structure. Figure 2 describes also the differences in the kinetics of the microstructure changes between hydrous titania containing 10% ruthenia and hydrous titania observed by ETA during heating. In the temperature interval 60–230°C a more intense initial increase of radon release rate E was observed for hydrous titania containing 10% ruthenia (dotted line, Fig. 2) as compared to hydrous titania. As confirmed by TG results [32] the increase of E corresponded to the liberation of the surface ini-

tially covered by water molecules, reflecting the formation of water free surface, due to the dehydration of the sample.

The onset of the crystallisation was determined at 400°C as the temperature of a change in the slope of the ETA curve. The crystallisation interval in the bulk was determined by DTA as 430–480°C. ETA results were in agreement with DTA, XRD patterns, the surface area measurements and TEM micrographs [32].

In the temperature range 830–1000°C, a more intense increase in E took place with the $(TiO_2)_{0.9}$–$(RuO_2)_{0.1}$ as compared to the titania sample (Fig. 2). The differences in the diffusion mobility of radon atoms reflected the different atomic transport properties of the respective samples in this temperature range. Moreover, the transport properties of the $(TiO_2)_{0.9}$–$(RuO_2)_{0.1}$ and its intermediate products prepared after heating to selected temperatures 380, 580 and 980°C were assessed using the values of the activation energy Q of radon diffusion determined from the plot log $(E–E_{25})$ *vs*. $(1/T)$. ETA results of the ruthenium containing titania based powders were quantitatively evaluated by means of the mathematical model and published in our study [33]. The results of the evaluation made it possible to predict the thermal behavior of these materials.

Characterisation of gels during their thermal treatment

Thermal behaviour of sol-gel prepared hydrous titania gel layers was studied by ETA, TG and DTA [34]. It was found that dehydration takes place in the temperature range 30–250°C followed by thermal decomposition of organic molecules remaining in the sample from Ti-*iso*-propoxide. Annealing of porosity and surface irregularities of dehydrated titania layers deposited on silica glass was indicated by ETA in the temperature range 255–440°C. The temperature of 500°C was recommended for the preparation of consolidated polycrystalline anatase layers [34].

ETA was used in the characterisation gelation processes [20]. Silicagel, xerogels of urania, titania, zirconia, alumina/SiC and others were advantageously investigated by ETA [20–22] under *in situ* conditions of ageing, drying, crystallisation or sintering. Ageing was indicated by a decrease of E, as a result of continuing polycondensation or re-precipitation of the gel network. During gel drying the increase of the radon release E was observed, indicating the removal of a liquid from the interconnected pore network. The removal of surface OH groups from pore network was reflected by an increase of radon release rate E, indicating increase of the surface area and nanoporosity. The removal of other volatiles, e.g. residues of gelation agents from the intermediate products of ceramics, was usually accompanied by an increase of E, the subsequent decrease in E indicated the decrease of surface area and nanoporosity taking place on heating.

ETA results characterising the differences in the behaviour of the urania xerogels caused by various concentrations of gelation additives, conditions of drying, by ageing, etc., were used in the preparation of urania ceramics [21].

In general, ETA was recommended as a suitable tool for monitoring changes of surface area and microporosity of materials under *in situ* conditions of their treatment. This method was successfully used for testing quality of intermediate and final products of ceramics and glasses prepared by various techniques, e.g. sol-gel, chemical vapour deposi-

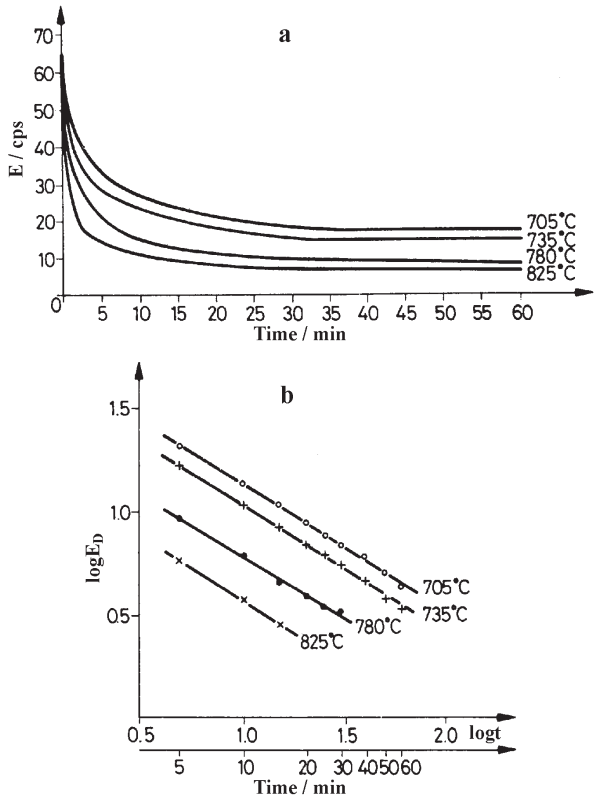

Fig. 3 ETA curves of ThO_2 (Ex-oxalate) during isothermal treatment in air at temperatures: 705, 735, 780, 825°C; a – values of emanation release rate E_{total} related to time; b – dependence $\log E_D = f(\log \text{time})$ where E_D are evaluated as $E_{total} - E_{25°}$ [37]

tion (CVD), physical vapour deposition (PVD), etc. ETA was also used for the determination of optimal temperature for thermal treatment of ZnS layers deposited by CVD on glass plates [35]. Both bulk samples, ultrafine powders, fibers, thin film coatings and membranes were characterized by ETA. Morphology developments of BC, BN and BCN based materials during heating of their precursors were monitored by ETA with the aim to obtain supplementary information about the thermal processes and the intermediate products formed during the preparation of the non-oxidic ceramics [36].

Kinetics study of surface and morphology changes of ceramic powders

It was demonstrated in a number of cases [1, 3, 19–22] that changes of surface area and morphology of ceramic powders can be characterised by ETA at *in situ* conditions of their treatment.

ETA results of thoria powder are demonstrated in Fig. 3, indicating the kinetics of the annealing of surface roughness and structure defects in the near surface layers. The kinetic parameters of this process taking place in the temperature interval 705–825°C were determined as follows [37].

$$\log S_{\text{eff}} = n\log t + constant \quad (7)$$

where n=0.64 and S_{eff} is the surface area reflected by the radon release measured in the respective temperature range.

Testing reactivity of powdered solids

A number of reactions between solid powders, e.g. $ZnO–Fe_2O_3$ [38], $BaCO_3–TiO_2$, $BaSO_4–TiO_2$ [39–40], have been studied by means of ETA. In the systematic study [38] of the reactivity of powder components in the $ZnO–Fe_2O_3$ system ETA made it possible to determine the initial stages of the solid state reaction and the formation of the ferrite structure, resp. DTA, dilatometry and X-ray diffraction used for comparison with ETA were not sensitive enough to indicate the initial reaction stage. The high sensitivity of ETA towards reaction between powders permitted the determination of the reactivities of the components used in various reaction mixtures [38, 41]. The reactivities of iron(III) oxide samples with various chemical and thermal histories, determined by ETA, agreed well with the results of other experimental techniques [4]. This method revealed differences in the reactivities of commercial iron(III) oxide samples, declared as identical when using traditional BET. surface area measurements [4]. The difference in the reactivities was checked by ETA during heat treatments of the reaction mixtures corresponding to the technological conditions of ferrite manufacture. ETA was also used in the characterisation of microstructure changes of intermediate products of high T_c superconducting ceramic materials e.g. Y–Ba–Cu–O [42, 43] and Bi–Ca–Sr–Cu–O [4]. Supplementary information on the reactivity of ceramic powders at *in situ* conditions of the solid-state reactions was obtained by ETA.

Thermal behaviour of glasses and their alteration products

Differences between surface and volume stages of the crystallisation and melting of glasses were revealed by means of ETA. The results obtained for the systems $PbO–SiO_2$ and Ge–Se–Te are presented in [44, 45].

This method has also found application in the field of the vitrification of hazardous waste, namely in the determination of optimal conditions for immobilisation of the waste containing Sr and Cs from nuclear power plants, and in testing durability of this glass towards hydrolytic corrosion [46–48].

Glasses designed for the vitrification of hazardous waste were characterised by means of ETA both as in virgin and altered forms. The annealing of surface roughness, sintering of virgin glass powder as well as the effect of mechanical polishing on

the surface roughness of silica glass plate were estimated by means of ETA. Moreover, the annealing of porosity of altered glass was characterised [48].

Thermal behaviour of clay minerals

Results of ETA characterising thermal behaviour of clay minerals, such as kaolinite [50], montmorillonite [51, 52], saponite, beidelite [51], goethite, and lepidocrocite [53] and others were in a good agreement with the results of DTA, TG, evolved gas analysis, etc. ETA was also used for the comparison of thermal behaviour of montmorillonite saturated with various cations [54]. The differences in the microstructure changes were observed in the temperature range where the crystallisation of dehydrated meta-montmorillonite takes place [54]. Moreover, the interaction of montmorillonite with organic substances, representing various types of pollutants of soils, was studied by means of ETA [55, 56]. A high sensitivity of ETA to changes in the surface layers of altered montmorillonite mineral samples was observed.

For vermiculite (locality Santa Ollaya, Spain) [57, 58] it was demonstrated by ETA that Na^+ ions and NH_4^+ ions have a significant effect on the microstructure changes taking place during the heat treatment of the natural Mg vermiculite samples saturated with these ions. The ETA made it possible to determine the temperatures of the onset of the collapse of inter-laminar space followed after the release of water molecules from Na^+ saturated and natural Mg vermiculite.

Effect of grinding on thermal behaviour of materials

The effect of grinding on the thermal behaviour titania [59], quartz [60], goethite [61] and others was investigated by ETA. ETA results were used for characterization of differences in thermal behaviour of goethite before and after grinding [61]. For a non-ground sample the dehydroxylation was characterised by the increase of the radon release rate, E, in the range from 230 to 290°C reflecting the formation of open pores. The decrease of E at temperatures from 290 to 800°C (Fig. 5 in [61]), indicated the annealing of porosity formed during the previous dehydroxylation of goethite. The increase of E, starting at about 800°C, was interrupted for the ground sample in the temperature range 950–1070°C, which was ascribed to the initial sintering of hematite particles. It was supposed that the grinding caused partial amorphisation of goethite, giving rise to structure defects and enhancing the sintering of ground particles.

Thermal behaviour of some organic compounds and polymers

Differencies in thermal behaviour of *ortho*-, *meta*- and *para*-barium benzoate were observed when measuring their emanating power [62]. Similarly, the microstructure of barium phtalate, *iso*-phalatate and *tere*-phatalate was assessed using emanating power measured in the range 25–100°C [63]. Consequently, it was supposed that the respective solid geometric isomers have differently packed lattices. ETA was used as

a complementary method to DTA, TG and MS in the investigation of thermal stability of complex metal compounds of transition elements containing various organic ligands. The information about temperature intervals of microstructure changes of the initial solid compounds and intermediate products of their heating was obtained from ETA results [64–68]. Phase transitions taking place on heating of caffeine were characterized by ETA, giving supplementary information to that obtained by DSC and XRD [69].

Low density polyethylene was characterized by means of ETA with the aim to assess the effect of electron beam irradiation of its thermal behavior [70]. It was found that after the electron beam irradiation, causing the cross linking of the polyethylene, the thermal stability of the polymer increased.

Hydration of cementitious binders

Morphology changes taking place during hydration reactions of tricalcium silicate ($3CaO{\cdot}SiO_2$) used as a Portland cement clinker mineral, as well as of cements with various mineralogical compositions were monitored by ETA [24]. The designed mathematical model [17] describing the morphology changes of cementitious binders was confirmed by experimental ETA results. The hydraulic reactivity of various cementitious binders was determined from ETA results in the early stages. Changes of surface and morphology taking place in the hydration products of Portland and slag cements, respectively have also been monitored by this method [71] under *in situ* conditions of the setting of the cement paste.

Characterisation of the barrier properties of protective coatings

The basic materials for the new protective coatings are hybrid materials, called ORMOCERs® (Organically Modified Ceramics) prepared by the sol-gel technique. Depending on the functionalities of the starting compounds, the ORMOCER® properties can be adjusted to particular requirements, such as, e.g. the good adhesion to corroded, uncorroded and patinated bronzes, long term stability against weathering and protection of the metal surface against the attack of water and pollutants.

In the Institute of Inorganic Chemistry, Academy of Sciences of the Czech Republic in cooperation with the Nuclear Research Institute Řež the samples of protective coatings were tested by means of ETA. ETA curves for two protective coatings are demonstrated in Figs 4a and b. The samples were measured before weathering (curves 2) and after weathering (curves 1) in a climatic chamber. From differences in ETA curves the effect of weathering on the barrier properties of the protective layers was assessed. Radon release measurements at room temperature and at elevated temperatures, resp., were used for the quantitative characterization of the protective coatings barrier properties. The radon diffusion coefficient D (20°C), calculated from the radon release rate measured at 20°C, reflects the protective properties of the coating layers. The activation energy Q of radon diffusion, calculated from the temperature

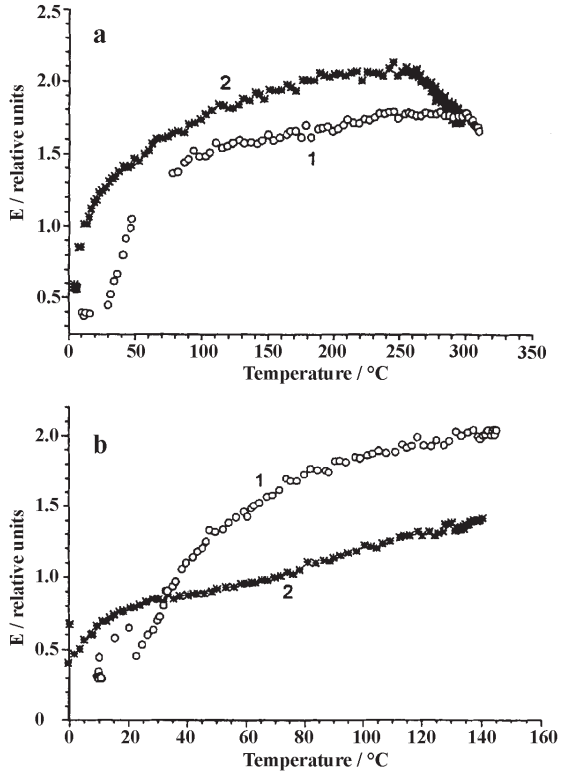

Fig. 4 Results of ETA measurements of weathered (curve 1) and non-weathered (curve 2) samples of ORMOCER® protective coatings. Heating in air at the rate 1 K min^{-1} was used; a – sample denoted ORMOCER® 9; b – sample denoted ORMOCER® 11 [72]

dependence of radon release rate, was used for the characterization of the radon migration controlled by diffusion in the protective coatings.

The radon diffusion characteristics were calculated [72] from ETA heating curves, according to the expression (8)

$$E_D = \tan hAl/Al \quad (8)$$

where E_D is the radon release rate due to diffusion, the constant $A=(\lambda_{Rn}/D)^{1/2}$.

$D=D_0=\exp(-Q/\boldsymbol{RT})$, l is the thickness of the coating layer, λ_{Rn} is the radon decay constant, equalling (ln2/55.6), $\boldsymbol{R}$ is the molar gas constant, equaling 1.99 cal s^{-1}.

The radon diffusion parameters for the protective layers, calculated from ETA curves, are summarised in Table 1. The main parameters used for the quantitative characterisation of the barrier properties are:

- coefficient of radon diffusion at 20°C, D (20°C)
- activation energy Q of radon diffusion, and
- pre-exponential factor D_0.

Table 1 Radon diffusion characteristics of weathered and non-weathered protective coatings

Notation of the sample	Sample treatment	D_0/cm^2 s^{-1}	Activation energy Q of Rn diffusion/ kcal mol^{-1}	D (20°C)/cm^2 s^{-1}
OR9	weathered	$2.19 \cdot 10^{-3}$	7.944	$2.83 \cdot 10^{-9}$
OR9	non-weathered	$2.59 \cdot 10^{-4}$	4.080	$42.45 \cdot 10^{-7}$
OR11	weathered	$4.26 \cdot 10^{-2}$	10.013	$1.62 \cdot 10^{-9}$
OR11	non-weathered	$7.72 \cdot 10^{-4}$	7.13	$7.65 \cdot 10^{-8}$

A good correspondence of the experimental and theoretic curves, obtained as a result of mathematical modelling was found. ETA was recommended for the characterization of the barrier properties of coated samples after their exposure to varying weathering conditions and for the investigation of the kinetics of the aging and microstructure changes of the protection layers.

Emanation thermal analysis in perspective

ETA has become an internationally recognised tool in material chemistry and material science. The most advantageous applications of ETA were reported in the field of advanced materials with tailored properties, e.g. characterisation of thermal behaviour of solid precursors of the advanced ceramic materials in the form of films, bulk or nano-structure particles. The chemical and thermal durability of the advanced materials were also tested by ETA. It contributed to the design of anticorrosion protection layers, in the preparation of catalysts, novel materials with photosensitive properties, advanced ceramic materials, in the characterisation of ceramic and glassy matrices for the immobilisation of high level radioactive waste, in the diagnostics of near surface layers of the industrially produced FLOAT glass, the characterisation of clay minerals and products of their alteration by environmental pollutants, etc.

Several research teams have been recently co-operating with the Nuclear Research Institute Řež using emanation thermal analysis in the frame of national and international projects sponsored e.g. by the Grant Agency of the Czech Republic, the Ministry of Education of the Czech Republic, the International Atomic Energy Agency (IAEA), by the German Ministry of Education and Research, by the European Union (EU-PECO Program), the US–Czech Science and Technology fund, the US Agency for International Development, the Science and Technology Agency of Japan.

The Nuclear Research Institute, Řež in co-operation with the Institute of Inorganic Chemistry, Academy of Sciences of the Czech Republic, the National Institute for Materials Science, Tsukuba, Japan, the Moscow State University, Russia, and the University of Košice, Slovak Republic, are continuing to develop and use the emanation thermal analysis. As it follows from this review, ETA is ready to fulfill the future needs of the materials characterization and to contribute to the solution of practical tasks.

This publication was prepared in the framework of the Project No. LN00A028 supported by the Ministry of Education of the Czech Republic. The authors would also like to acknowledge the support obtained by the Ministry of Education of the Czech Republic in the frame of the KONTAKT program (Project Nos ME 180 and ME 235).

References

1 V. Balek and J. Tölgyessy, Emanation thermal analysis and other radiometric emanation methods, in Wilson and Wilson (Eds), Comprehensive Analytical Chemistry, Part XIIC, Elsevier, Amsterdam 1984, p. 304.
2 J. F. Ziegler and J. P. Biersack, The stopping and ranges of ions in solids, Pergamon Press, New York 1985.
3 W. D. Emmerich and V. Balek, High Temp.-High Pressures, 5 (1973) 67.
4 V. Balek, J. Thermal Anal., 35 (1989) 405.
5 J. Kří and V. Balek, Thermochim. Acta, 71 (1983) 175.
6 J. Kří and V. Balek, Thermochim. Acta, 78 (1984) 377.
7 V. Balek and J. Kří , Thermochim. Acta, 81 (1981) 335.
8 J. Kří , V. Balek and I. N. Beckman, Thermochim. Acta, 92 (1985) 101.
9 I. N. Beckman, A. A. Shviryaev and V. Balek, Thermochim. Acta, 104 (1986) 255.
10 A. A. Shviryaev, I. N. Beckman and V. Balek, Thermochim. Acta, 111 (1987) 215.
11 J. Kří and V. Balek, Thermochim. Acta, 120 (1987) 241.
12 J. Kří and V. Balek, Thermochim. Acta, 110 (1987) 245.
13 V. Balek and I. N. Beckman, Thermochim. Acta, 318 (1998) 221.
14 V. Balek and I. N. Beckman, Thermochim. Acta, 295 (1997) 147.
15 I. N. Beckman and V. Balek, J. Therm. Anal. Cal., 55 (1999) 123.
16 I. N. Beckman and V. Balek, J. Therm. Anal. Cal, 67 (2002) 49.
17 V. Balek and I. N. Beckman, J. Therm. Anal. Cal, 67 (2002) 37.
18 M. D. Norgett and H. B. Lidiard, Phil. Mag., 18 (1968) 1193.
19 V. Balek and M. E. Brown, Less common techniques, In: Handbook on Thermal Analysis and Calorimetry, Vol. 1, Chapter 9. Ed. M. E. Brown, Elsevier Science B.V., 1998, pp. 445–471.
20 V. Balek, Z. Málek and H. J. Pentinghaus, J. Sol-gel Sci., Technol., 2 (1997) 301.
21 V. Balek, M. Vobořil and V. Baran, Nucl. Technol., 50 (1980) 53.
22 V. Balek, E. Klosová, M. Murat and N. Almeida Camargo, Bull. Amer. Cer. Soc., 75 (1996) 73.
23 V. Balek, Thermochim. Acta, 72 (1984) 147.
24 V. Balek and J. Dohnálek, J. Mater. Sci., 17 (1982) 2281.
25 C. Jech and R. Kelly, Proc. Br. Ceram. Soc., 9 (1976) 359.
26 F. W. Felix and K. Meier, Phys. Status Solidi, 32 (1969) 139.
27 R. Kelly and Hj. Matzke, J. Nucl. Mater., 17 (1965) 197.
28 R. Kelly and Hj. Matzke, J. Nucl. Mater., 20 (1966) 175.
29 V. Balek, J. Mater. Sci., 5 (1979) 166.
30 V. Balek, V. Zeleňák, T. Mitsuhashi, S. Bakardjieva, J. Šubrt and H. Haneda, J. Therm. Anal. Cal., 67 (2002) 83.
31 T. Mitsuhashi, A. Watanabe, V. Balek, E. Klosová, J. Málek, J. Šubrt and V. Štengl, Materials Letters, 39 (1999) 46.

32 V. Balek, E. Klosová, J. Málek, J. Šubrt, J. Boháček, A. Watanabe and T. Mitsuhashi, Thermochim. Acta, 340–341(1999) 301.
33 V. Balek, V. Zeleňák, T. Mitsuhashi, I. N. Beckman, H. Haneda, and P. Bezdička, J. Therm. Anal. Cal, 67 (2002) 63.
34 V. Balek, E. Klosová, N. Sumi, T. Mitsuhashi and J. Šubrt, Thin Solid Films, 394 (2001) 443.
35 V. Balek, J. Fusek, O. Kří , M. Leskelä, L. Niinistö, E. Nykänen, J. Rautanen and P. Soininen, J. Mater. Res., 9 (1994) 119.
36 T. Sato, M. Hubáček, V. Balek, J. Šubrt, O. Kří and T. Mitsuhashi, J. Therm. Anal. Cal., 60 (2000) 661.
37 V. Balek, J. Mat. Sci., 17 (1982) 1269.
38 V. Balek, J. Am. Ceram. Soc., 53 (1970) 540.
39 T. Ishii, Thermochim. Acta, 88 (1985) 27.
40 T. Ishii, Thermochim. Acta, 109 (1979) 252.
41 V. Balek, J. Appl. Chem. (London), 20 (1970) 73.
42 V. Balek and J. Šesták, Thermochim. Acta, 133 (1988) 23.
43 V. Balek and P. K. Gallagher, Thermochim. Acta, 186 (1991) 1479.
44 V. Balek and J. Götz, in J. Götz (Ed.), Proc. 11th Int. Glass Congress, Prague 1977, Vol. 3, p. 35.
45 S. Bordas, M. Clavaguera-Mora and V. Balek, Thermochim. Acta, 93 (1985) 283.
46 V. Balek, T. Banba, I. N. Beckman, Z. Málek and J. Šubrt, J. Therm. Anal. Cal., 60 (2000) 989.
47 V. Balek, Z. Málek and A. Clearfield, In: Proc. 7th Int. Conference on high level radioactive waste management, Las Vegas, Nevada 1996, p. 474.
48 V. Balek, Z. Málek and A. Clearfield, In: Proc. of an International Workshop 'Glass as a waste from and vitrification technology', NAS, Washington D. C. (NRS Paper E.58) p. 102.
49 N. H. Menzler, N. Mörtel, R. Weissman and V. Balek, Glass Technol., 40 (1999) 65.
50 V. Balek and M. Murat, Thermochim. Acta 282/283 (1996) 385.
51 Z. Málek, V. Balek, D. Garfinkel-Shwekey and S. Yariv, J. Thermal Anal., 48 (1997) 83.
52 V. Balek, Z. Málek and E. Klosová, J. Therm. Anal. Cal., 53 (1998) 625.
53 V. Balek and J. Šubrt, J. Pure and Appl. Chem., 67 (1995) 1839.
54 V. Balek, Z. Málek, S. Yariv and G. Matuschek, J. Therm. Anal. Cal., 56 (1999) 67.
55 V. Balek, K. Györyová, L. Kelnar and W. Smykatz-Kloss, Appl. Clay Sci., 7 (1992) 179.
56 V. Balek, Z. Málek, U. Ehrlicher, K. Györyová, G. Matuschek and S. Yariv, Appl. Clay Sci., in print.
57 J. Poyato, L. A. Perez-Maqueda, A. Justo and V. Balek, Clay and Clay Min, submitted.
58 J. Poyato, L.A. Perez-Maqueda, M. C. Jimenez de Haro, J. L. Perez-Rodriguez, J. Šubrt and V. Balek, J. Therm. Anal. Cal., 67 (2002) 73.
59 C. Real, J. M. Criado and V. Balek, J. Mat. Sci., 33 (1998) 5247.
60 V. Balek, J. Fusek, O. Kří and M. Murat, Thermochim. Acta, 262 (1995) 209.
61 L. A. Perez-Maqueda, J. Šubrt, V. Balek, J. M. Criado and C. Real, J. Therm. Anal. Cal., 60 (2000) 997.
62 V. Balek, F. Charbonnier and P. Bussiere, J. Thermal Anal., 7 (1975) 51.
63 V. Balek and J. Kroupa, Thermochim. Acta, 22 (1978) 157.
64 V. Balek and K. Györyová, Thermochim. Acta, 179 (1991) 109.
65 K. Györyová and V. Balek, J. Thermal Anal., 38 (1992) 789.
66 K. Györyová and V. Balek, J. Thermal Anal., 40 (1993) 519.

67 K. Györyová, V. Balek, B. H. Behrens, G. Matuschek and A. Kettrup, J. Thermal Anal., 48 (1997) 1263.
68 K. Györyová, V. Balek and V. Zeleňák, Thermochim. Acta, 234 (1994) 221.
69 M. Epple, H. K. Cammenga, S. M. Sarge, R. Diedrich and V. Balek, Thermochim. Acta, 250 (1995) 29.
70 I. N. Beckman and V. Balek, Thermochim. Acta, 320 (1998) 169.
71 V. Balek and J. Dohnálek, Cem. and Concr., Res., 22 (1992) 459.
72 V. Balek, Z. Málek, B. Čásenský, D. Ni ňanský, J. Šubrt, E. Večerníková, H. Römich and M. Pilz, J. Sol-gel Sci. Technol., 8 (1997) 591.